Modulation of band structure in wurtzite ZnO via site-selective Ga–N codoping

2006 J. Phys.: Condens. Matter 18 6281

(http://iopscience.iop.org/0953-8984/18/27/011)

INSTITUTE OF PHYSICS PUBLISHING JOURNAL OF PHYSICS: CONDENSED MATTER

J. Phys.: Condens. Matter **18** (2006) 6281–6287 doi:10.1088/0953-8984/18/27/011

Modulation of band structure in wurtzite ZnO via site-selective Ga–N codoping

C J Zhou and J Y Kang[1]

Department of Physics and Semiconductor Photonics Research Centre, Xiamen University, Xiamen 361005, People's Republic of China

E-mail: zhoucj@xmu.edu.cn and jykang@xmu.edu.cn

Received 16 March 2006, in final form 3 June 2006
Published 23 June 2006
Online at stacks.iop.org/JPhysCM/18/6281

Abstract

We investigated the electronic structures of two Ga–N codoping isoelectronic configurations in wurtzite ZnO by means of first-principles calculations. The calculated total energies show that both the isoelectronic configurations are stable in ZnO. This result is attributable to the strong hybridization between the Ga 3d and N 2p states. The polarization is significantly changed and the top of the valence band is substantially split up towards the conduction band in a site-selective isoelectronic configuration, which causes a reduction of the activation energy of the N related acceptor and thus enhances the hole concentration by more than three orders of magnitude.

1. Introduction

ZnO has become a promising material for ultraviolet light emitting diodes and lasers, and transparent high power electronic devices due to the wide direct band gap and large exciton binding energy [1]. In order to fabricate ZnO-based optoelectronic devices, both n- and p-type ZnO are needed. Undoped ZnO exhibits n-type conductivity, and it is, therefore, difficult to achieve p-type ZnO because acceptors are compensated by various native donors, such as oxygen vacancies, Zn interstitials, and other donors [2]. Among group V dopants, N is considered to be a shallow acceptor compared to P and As [3]. However, there are still many difficulties in using N as a dopant. Doping with a pure nitrogen source leads to n-type conductivity, while doping with a NO_2 or NO source does lead to p-type behaviour, which however, tends to revert to n-type behaviour over time [4, 5]. According to these observations, it appears that N_O acceptors are not be stable and will be compensated in ZnO. Theoretical and experimental research suggested that N_O acceptors have a large activation energy [3, 6] which may also limit the formation of acceptors. Yamamoto *et al* have reported a codoping method for fabricating p-type ZnO with III–N codoping [7]. However, this codoping theory is not site

[1] Author to whom any correspondence should be addressed.

selective and therefore cannot give the detailed electronic distributions and band structures for different site-selective codoping configurations. That is probably why some experiments could obtain p-type ZnO by codoping N with Ga [8], but others could not [9].

The III–N codopants can form isoelectronic defects in ZnO. N and Ga impurities usually substitute for the host O and Zn atoms, respectively, and their valence difference will form a local polarity. Different site-selective isoelectronic Ga–N configurations influence the local polarization of wurtzite ZnO. Since the polarization is one of the important factors that determine the properties of wurtzite ZnO, the understanding of the site-selective codoping effects on electronic structures of wurtzite ZnO is worth detailed study.

2. Calculation details

The first-principles calculations were carried out with a package called VASP (Vienna *ab initio* simulation package) [10–12]. The wavefunctions are expressed as a supposition of plane waves with a cut-off energy 395.99 eV. Ionic potentials are represented by ultrasoft pseudopotentials with the Perdew–Wang 1991 (PW91) GGA (generalized gradient approximation) correction [13, 14]. For valence electrons, the outermost s, p, and d states of Zn and Ga atoms, s and p states of O and N atoms are employed in the work. And a 64-atom supercell was used to calculate the electronic structures of undoped, N monodoped and site-selective Ga–N codoped ZnO. There are two Ga–N codoping configurations. While fixing a Ga impurity at a substitutional Zn site, we put a N impurity at the first-nearest-neighbour above (configuration II) and below (configuration I) the Ga atom, as shown in figure 1(a). The underling motives for these two codoping configurations are: (1) the formation of Ga–N pair is energetically favourable in ZnO crystal and (2) the practical growth direction is along the *c*-axis. In addition, all four cases were relaxed and optimized to ensure the correctness of the calculation results.

3. Results and discussion

In order to ascertain the site-selective Ga–N codoping stability the defect energies of the Ga monodoped, N monodoped, and site-selective Ga–N codoped ZnO were calculated and compared; these are defined as the differences between the total energies with and without a defect. The defect energy of the N monodoped configuration is $\Delta E_{T-\mathrm{N}} = 1.22$ eV. Therefore, it is difficult to substitute N for O. Even $\mathrm{N_O}$ has been formed somehow in practice; it cannot be stable in ZnO for long. These calculation results agree well with the experimental results reported previously [4, 5]. Fortunately, the defect energies of the Ga–N codoped configurations I and II are $\Delta E_{T-\mathrm{I}} = -2.89$ eV and $\Delta E_{T-\mathrm{II}} = -2.84$ eV, respectively, which are also lower than the $\Delta E_{T-\mathrm{Ga}} = -1.85$ eV of the Ga monodoped configuration. In both Ga–N codoped configurations, the Ga atom substituting for a Zn atom causes the nearest neighbouring O and N atoms to relax inward for about 3.7% and 6.8%, respectively. This shows that the site-selective Ga–N codoping can easily form in the ZnO crystal and exist stably.

To understand the variations of the different site-selective Ga–N codopants, we introduce the induced charge density difference $\Delta\rho$ via

$$\Delta\rho = \left(\rho_{\mathrm{ZnO:(Ga,N)}} - \rho_{\mathrm{ZnO}}\right) - \left(\rho_{\mathrm{ZnO:Ga}} - \rho_{\mathrm{ZnO}}\right) - \left(\rho_{\mathrm{ZnO:N}} - \rho_{\mathrm{ZnO}}\right), \tag{1}$$

where $\rho_{\mathrm{ZnO:(Ga,N)}}$, $\rho_{\mathrm{ZnO:Ga}}$, $\rho_{\mathrm{ZnO:N}}$, and ρ_{ZnO} are the charge densities of Ga–N codoped, Ga monodoped, N monodoped, and undoped ZnO, respectively. Since the atoms adjust their positions automatically in the self-consistent calculation with lattice relaxations, it is in general impossible to compare the charge density data in the same spatial positions among those of the

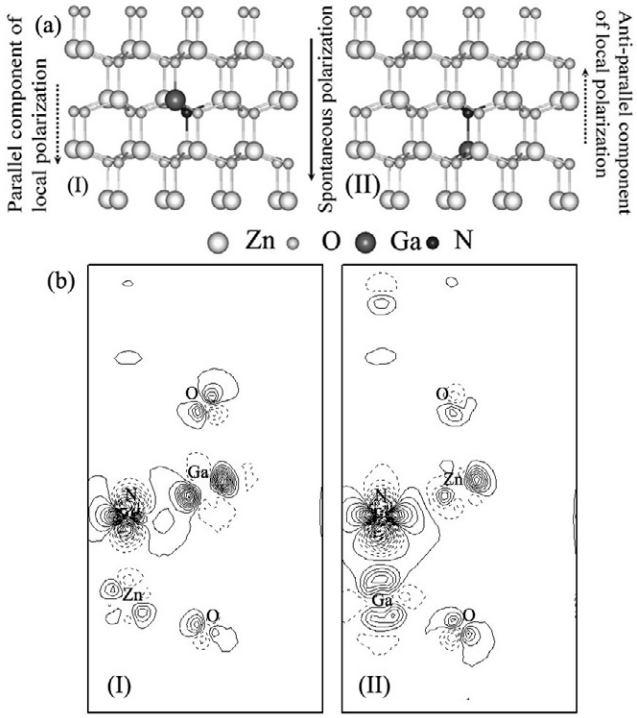

Figure 1. (a) Crystal structures of configurations I and II for Ga–N codoped wurtzite ZnO. The spontaneous polarization orientation and the local polarization components are marked with solid and dashed arrows, respectively. (b) Charge density differences on a cross section containing Ga and N atoms plotted for configurations I and II. Regions of increased and decreased charge density are represented by solid and dashed lines, respectively.

different dopants if relaxations are allowed. For this reason, figure 1(b) shows $\Delta\rho$ on a vertical plane containing the Ga and N atoms from the data calculated via equation (1) but without lattice relaxation. The charge density around the N atom redistributes mainly by decreasing in the vertical direction. But the charge density of the Ga atom increases mainly in the direction of the Ga–N bond. It is known that the charge density depends on the outermost electrons. The outermost electrons used in this work are 4s, 4p, and 3d states for the Ga atom, and 2s and 2p states for the N atom. Since the s state has spherical symmetry, we suggest that the induced charge density redistributions above are associated with p and d states. The dominant charge variations around the N atom are attributable to a depopulation of a p_z-like state and a population of a p_y- or p_x-like state due to the interaction with the Ga codopant. On the other hand, the charge variations around the Ga atom are mainly attributable to d_{yz}-like and d_{zz}-like states of the Ga atom. Therefore, there is a hybridization between the Ga 3d and N 2p states, which can explain the lowering of the total energies, as mentioned above. The hybridization is stronger in configuration II than that in configuration I because the negative charges of the Ga atom and the positive charges of the N atom align in a line with the *c*-axis and thus influence the crystal field much more significantly in that direction.

The energy band structures are clearly influenced by the different local crystal fields in configurations I and II. Although Ga acts as a donor in both configurations, the main differences appear at the tops of the valence bands. The twofold-degenerate Γ_{5v} level at the top of the

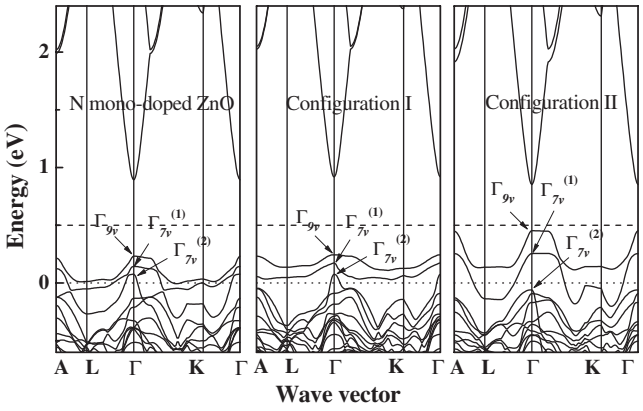

Figure 2. Energy band structures of N monodoped ZnO, Ga–N codoped configurations I and II. The dashed line in the band gap is assumed to be an N acceptor level and the dotted line denotes the twofold-degenerate Γ_{5v} level of the top of the valence band for undoped ZnO.

valence band of undoped ZnO splits into Γ_{9v} and $\Gamma_{7v}^{(1)}$ levels, which shifts into the band gap and the separation between them and the non-degenerate Γ_{1v} level (labelled as $\Gamma_{7v}^{(2)}$ here) broadens upon N monodoping, as shown in figure 2. The splitting and shifts are more distinct for both codoping configurations, especially for configuration II. Because the spin–orbit interaction is not taken into account in our calculation, the difference of the splitting energy is related to the difference in crystal field between configurations I and II. It is known that the nearby Ga–N pair is isoelectronic in ZnO. However, the local positive charge centre formed by N_O and the local negative charge centre formed by Ga_{Zn} generate a local polarized field, which can be decomposed into two components, one along the *c*-axis and the other perpendicular to it. Since the spontaneous polarization direction is also along the *c*-axis in the ZnO host crystal, the component along the *c*-axis plays an important role in the splitting and shifts of the tops of the valence bands. The component along the *c*-axis is estimated to be -1.87 electron Å for configuration II and $+0.62$ electron Å for configuration I, where $-$ and $+$ correspond to the local polarizations antiparallel and parallel with the spontaneous polarization, respectively. On the basis of the above analysis, we conclude that the larger energy splitting and shifts are mainly attributable to the larger component along the *c*-axis of the local polarization in configuration II.

In addition to the splitting of the top of the valence band, the lineshape of the valence band edge is also changed significantly. For electronic devices, the effective masses directly related to the lineshape of the valence band edge are especially important for analysing the device properties, particularly the current transport characteristics. To reveal the different influences of the local polarization on the lineshape of the valence band edge, the effective masses of the lowest conduction band (c1) and of the uppermost valence band (v1) were calculated along the three symmetry axes: Γ–A, Γ–M, and Γ–K. In table 1, we list the effective mass tensors represented by a transverse mass $m_\perp$ and a longitudinal mass $m_\parallel$. The effective masses are highly anisotropic. The electron effective masses in undoped ZnO are $m_{c1,\perp} = 0.25\ m_0$ and $m_{c1,\parallel} = 0.17\ m_0$ where m_0 is the mass of a free electron, which agrees well with the results of local density approximation (LDA) calculation [15] and the experiments on cyclotron resonance [15] and photoreflectivity [16]. The hole effective masses are much larger than the electron effective masses which indicates that the holes are much heavier than the electrons in undoped ZnO crystal. This is in line with the experimental findings: that carriers in ZnO are dominated by electrons and the mobility of holes is much lower than that of electrons. The

Table 1. Effective masses calculated from undoped, N monodoped ZnO, and Ga–N codoped configurations I and II.

Mass (m_0)	Undoped	N monodoped	Configuration I	Configuration II
$m_{c1,\parallel}$	0.17	0.17	0.17	0.17
$m_{c1,\perp}$	0.25	0.25	0.25	0.25
$m_{v1,\parallel}$	3.12	8.76	11.80	45.63
$m_{v1,\perp}$	2.87	0.40	3.29	0.36
m_h^*	2.95	0.58	4.33	0.54

hole effective masses are very anisotropic for all configurations. The two components of the mass tensors become larger for configuration I compared to undoped and N monodoped ZnO. For configuration II although the longitudinal mass $m_{v1,\parallel}$ also becomes larger, the transverse mass $m_{v1,\perp} = 0.36\, m_0$ becomes much smaller than those of other configurations. To facilitate comparison, the average hole effective mass for conductivity m_h^* is given by

$$1/m_h^* = (1/3)(1/m_{v1,\parallel} + 2/m_{v1,\perp}). \tag{2}$$

Then the calculated value of $m_h^* = 0.54\, m_0$ for configuration II is much lower than that of configuration I, which means that the hole mobility in configuration II will be enhanced. As a result, the lineshapes of the valence band edge are also significantly influenced in different site-selective codoping configurations due to the different components of the local polarization along the c-axis. According to the analysis above, we believe that the energy band structure can be modulated by this kind of site-selective codoping.

In order for us to understand the contributions of different atoms to the shifts of the tops of the valence bands, the total and partial DOS were calculated, as shown in figure 3. Compared with the total DOS of undoped ZnO, the splitting band produces dense states around the valence band edge for both Ga–N codoped configurations. This enhances the electron transition probability from the N acceptor level to the valence band. Further examining the role of each atom from the partial DOS, the N 2p states are much higher around the valence band edge compared to O 2p, Zn 3d and Ga 3d states. But for the bottom of the conduction band, the Ga 4s states contribute more than the Zn 4s states do. Then the shifts of the N 2p states are strongly due to the hybridization between the Ga 3d and the N 2p states, consistent with the charge density redistribution. From this point of view, the hybridizations between the Ga 3d and N 2p states and the change of polarization play an important role in the splitting and shifts of the top of the valence band.

The hole concentration for partially compensated semiconductors is approximately given by

$$p \propto \exp(-\Delta E_A/kT). \tag{3}$$

Here ΔE_A is the thermal activation energy of the acceptor [17]. Although no impurity band is visible in the calculated energy bands of N monodoped ZnO, in practice there are acceptor levels related to the N impurity. We approximate the N acceptor activation energy $\Delta E_{A-N} = 0.266$ eV measured for N doped ZnO [18] as the energy difference between the N acceptor level and the top of the valence band of N monodoped ZnO, which is shown by dashed lines in figure 2. To simplify the comparison of numerical results, we assume that the N acceptor level does not follow the valence band but pins to the vacuum level. Since the isoelectronic Ga–N pairs only bring on the splitting of the top of the valence band by changing the local polarization and do not contribute to the conductivity, the energy differences between the additional N_O acceptor level and the top of the valence band are $\Delta E_{A-II} = 0.045$ eV

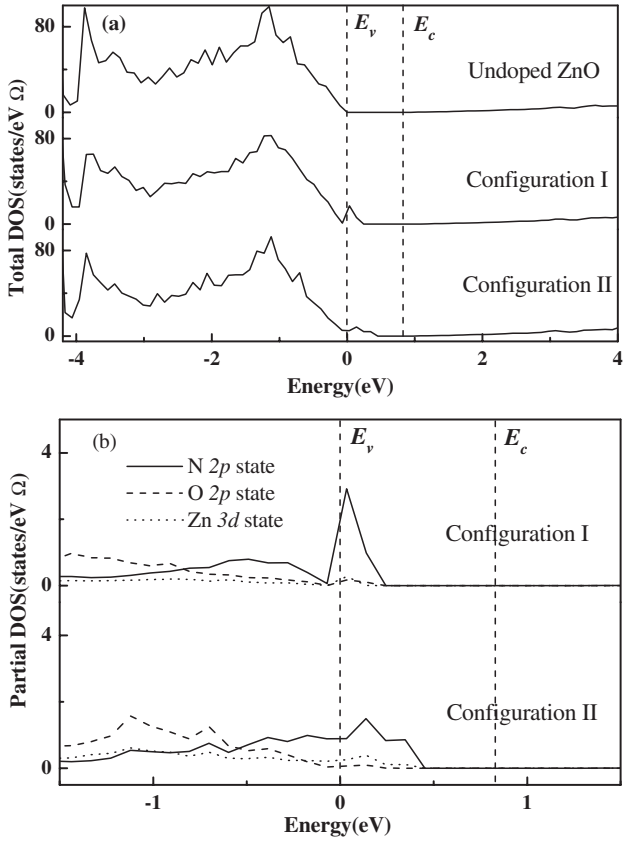

Figure 3. Total (a) and site-decomposed DOS (b) of undoped ZnO, Ga–N codoped configurations I and II. The top of the valence band and the bottom of the conduction band of undoped ZnO are marked by the dashed lines and denoted as E_v and E_c, respectively.

under the modulation of configuration II and $\Delta E_{A-I} = 0.254$ eV under the modulation of configuration I. Assume p_N is the hole concentration in N monodoped ZnO, p_I and p_{II} are the hole concentrations of the additional N_O acceptor under the modulation of configurations I and II, respectively. Then their ratios at room temperature according to equation (3) are approximately $p_I/p_N \propto \exp(-\Delta E_{A-I}/kT)/\exp(-\Delta E_{A-N}/kT) \approx 1.59$ and $p_{II}/p_I \propto \exp(-\Delta E_{A-II}/kT)/\exp(-\Delta E_{A-I}/kT) \approx 3.1 \times 10^3$. These estimated values show that the hole concentrations under the modulation of configuration I and in N monodoped ZnO have the same magnitude which is due to the fact that the splitting and shifts for these two configurations are close. However, the hole concentration under the modulation of configuration II is three orders of magnitude higher than that of configuration I. These results indicate that the hole concentration is enhanced by lowering the activation energy of the N acceptor under the local polarization field in configuration II.

4. Conclusions

In summary, the computation results for the total energy show that the site-selective isoelectronic Ga–N pair can exist stably in ZnO crystal due to the hybridization between the Ga 3d and N 2p states. Consequently, the polarization is significantly changed and causes

the top of the valence band to split substantially up towards the conduction band. The hole concentration under the modulation of configuration II is thus enhanced by more than three orders of magnitude due to lowering the activation energy of the N acceptor. Recent experiments showed a reasonable method for achieving this configuration in practice. Look *et al* and Guo *et al* have shown that the polarity of ZnO plays an important role in the impurity doping and that the p-type conductivity forms favourably in ZnO films grown on Zn polar surfaces [19, 20]. Furthermore, Iwai *et al* have obtained a high hole concentration and a lower acceptor activation energy for p-type GaN by introducing a δ doping where Mg was supplied in one pulse and then this was followed by a Si pulse during crystal growth in the [0001] direction [21]. By suitable control of the growth process, the site-selective Ga–N codoping in configuration II can be accomplished under the layer-by-layer and Zn polar growth conditions by δ doping.

Acknowledgments

The authors would like to express thanks to Dr Hui Fang of Xiamen University for helpful discussions. This work was partly supported by the Special Funds for Major State Basic Research Projects (Grant No 001CB610505), the National Natural Science Foundation (Grant No 60376015, 90206030, 60336020, and 10134030), grants from the Ministry of Education, and Fujian Province (2004H054 and E0410007) of China.

References

[1] Pearton S J, Norton D P, Ip K, Heo Y W and Steiner T 2004 *J. Vac. Sci. Technol.* B **22** 932–48
[2] Lee E C, Kim Y S, Jin Y G and Chang K J 2001 *Phys. Rev.* B **64** 085120
[3] Park C H, Zhang S B and Wei S H 2002 *Phys. Rev.* B **66** 073202
[4] Barnes T M, Olson K and Wolden C A 2005 *Appl. Phys. Lett.* **86** 112112
[5] Wang L G and Zunger A 2003 *Phys. Rev. Lett.* **90** 256401
[6] Wang L and Giles N C 2004 *Appl. Phys. Lett.* **84** 3049
[7] Yamamoto T and Katayama-Yoshida H 1999 *Japan. J. Appl. Phys.* **38** L166–9
[8] Joseph M, Tabata H and Kawai T 1999 *Japan. J. Appl. Phys.* **38** L1205–7
[9] Nakahara K, Takasu H, Fons P, Yamada A, Iwata K, Matsubara K, Hunger R and Niki S 2001 *Appl. Phys. Lett.* **79** 4139–41
[10] Kresse G and Furthmuller J 1996 *Phys. Rev.* B **54** 11169–86
[11] Kresse G and Furthmuller J 1996 *Comput. Mater. Sci.* **6** 15–50
[12] Kresse G and Joubert D 1999 *Phys. Rev.* B **59** 1758–75
[13] Perdew J P, Chevary J A, Vosko S H, Jackson K A, Pederson M R, Singh D J and Fiolhais C 1992 *Phys. Rev.* B **46** 6671–87
[14] Wang Y and Perdew J P 1991 *Phys. Rev.* B **44** 13298–307
[15] Oshikiri M, Imanaka Y, Aryasetiawan F and Kido G 2001 *Physica* B **298** 472–6
[16] Syrbu N N, Tiginyamu I M, Zalamai V V, Ursaki V V and Rusu E V 2004 *Physica* B **353** 111–5
[17] Kireev P S 1978 *Semiconductor Physics* ed M Samokhvalov (Moscow: MIR) pp 197–221
[18] Tamura K, Makino T, Tsukazaki A, Sumiya M, Fuke S, Furumochi T, Lippmaa M, Chia C H, Segawa Y, Koinuma H and Kawasaki M 2003 *Solid State Commun.* **127** 265–9
[19] Look D C, Reynolds D C, Litton C W, Jones R J, Eason D B and Cantwell G 2002 *Appl. Phys. Lett.* **81** 1830–2
[20] Guo X L, Choi J H, Tabata H and Kawai T 2001 *Japan. J. Appl. Phys.* **40** L177–80
[21] Iwai S, Hirayama H and Aoyagi Y 2002 *Defect and Impurity Engineered Semiconductors and Devices III* ed S Ashok, J Chevallier, N M Johnson, B L Sopori and H Okushi (Warrendale, PA: MRS) p 132